THE APPLICATION OF DUFFING'S EQUATION IN PREDICTING THE EMISSION CHARACTERISTICS OF SAWDUST PARTICLES

T.A.O. Salau[1], S.A. Oke[2]

ABSTRACT

Sawdust particles soon after emission from the cutting machine usually move dynamically with transformation in some dimensions. This paper models the sawdust particle motion as a two dimensional transformation system of continuous time series. Cost could be saved using this approach instead of utilizing dynamic systems that depend on time history. Two-dimensional graphical representation of continuous time series of Duffing's dynamic system for sawdust particles was investigated with emphasis placed on application to sawdust particle motion and the saw machines. Preliminary studies were made using the harmonic functions, F(t) = Cos(ωt) and F(t) = Sin(ωt), for their familiarity in both science and technology communities. The solution to Duffing's model equation for the sawdust particles was sought from displacement and velocity perspectives, using the Runge-Kutta Algorithm. Linear transformation that guarantees non-negative values of time series was implemented. This was followed by the respective computation of the x- and y-components of the resulting time series values of the sawdust movement using a 2π modulated time measured in radians. The graphical representations of the x- and y-components compared well quantitatively and qualitatively with the corresponding phase plots. The feasibility of modelling sawdust dynamics as emission from band saws was therefore demonstrated here, in approaches that thus advance knowledge of sawdust emission studies.

KEYWORDS: Sawdust Emission, Duffing's Dynamic System, 2-D Graphs, Sawmill

1.0 NOMENCLATURE

t	Time, in seconds
$F(t)$	Time series, in metres or metres per second
ω	Angular frequency, in radians per second
π	Constant, being 3.142
x	Duffing oscillator/sawdust particle displacement relative to a specified origin, in metres
$\dot{x}$	Duffing oscillator/sawdust particle velocity, in metres per second
$\ddot{x}$	Duffing oscillator/sawdust particle acceleration, in metres per second squared
γ	damping coefficient per second
P_o	Forcing amplitude coefficient, in metres per second squared
x_1	Equivalent representation of Duffing oscillator/sawdust particle displacement relative to a specified origin in Metres
$\dot{x}_1$	Equivalent representation of Duffing oscillator/sawdust particle velocity relative to a specified origin in Metres per second
$\dot{x}_2$	Equivalent representation of Duffing oscillator/sawdust particle velocity relative to a specified origin in Metres per second
$\ddot{x}_2$	Equivalent representation of Duffing Oscillator/Sawdust particle acceleration relative to a specified origin in metre per second squared
r	Radius, in metres or metres per second square, depending on the time series transformed
θ	2π modulated product of ω and t, in radians
X	Component of transformed time series (in metres or metres per second) along the horizontal direction
Y or y	Component of transformed time series (in metres or metres per second) along the vertical direction
F_{min}	Minimum of the time series value (old or new)

[1]Department of Mechanical Engineering, University of Ibadan, Nigeria, Email: tajudeen_salau@yahoo.com
[2] Corresponding author, Department of Mechanical Engineering, University of Lagos, Nigeria, Email: sa_oke@yahoo.com

UNIVERSITY OF IBADAN LIBRARY

V_1, V_2, V_3 and V_4 Velocities
D_1, D_2, D_3 and D_4 Displacements

2.0 INTRODUCTION

Sawdust particles are products of timbers sawn into various sizes and shapes in the sawmill industries. They are dispersed as a result of the impacted forces on the contact point of the band saw and the sawn timber or plank. However, sawdust has been recognised as a potential source of methane, hexanal and carbon monoxide [Pier and Kelly (1977); Svedberg et al. (2004)] and a strong causal agent for respiratory diseases such as asthma and childhood cancer in the offspring of sawmill workers [Demers et al. (1997); Heacock (2000); Arif et al. (2003); Siracusa et al. (2007)]. Thus, these hazardous emissions in sawdust require intensive control and proper understanding of its movements in the sawmill environment. Despite the importance of sawdust motion in monitoring the health status of sawmill workers, it appears that no study has presented a detailed analysis of its dynamics soon after leaving the band saw.

In the process of sawing, wind blows the particles causing them to move at varying speeds depending on the individual weight and shape of each particle dispersed, and their interaction. With time, the emitted particles eventually form concentric bands, which in the event of high wind soon diffuse into smaller fractions as the condition may be. Sawdust particles move with dynamic motion that is largely dependent on the velocity of the winds, force applied by the band saw, the respective weight and shape of individual particles, and their interactions [Bello and Mijinyawa (2010)]. When sawdust is emitted from the band saw, it moves in the opposite direction to that of the sawn timber, as confirmed by the results of direct surveys by the authors of band saws at various sawmills in Lagos, Nigeria. The validations to these descriptions are discussed in this work.

A survey of the literature on emission works concerning sawdust particle modelling, and studies relevant to Duffing's theory, all show a conspicuous absence of models of sawdust particle emission using a transformation approach. This approach, which enables a 2-dimensional graphical representation of dynamic systems, considering motion of sawdust emission from band saws in a timeframe, has not been documented. Although extensive literature exists on solutions of the Duffing equation and only a scanning of the important relevant equations with which we could compare the current study are discussed here, to the best of the authors' knowledge, the approach reported here has not been attempted to solve the problem of the motion of sawdust concerning the motion of particles soon after their emission from the band saw. Ahmad et al. (2008) obtained a sequence approximate solution converging monotonically and quadratically to the unique solution of the forced Duffing equation with integral boundary conditions. The work did not address the practical application of the solution developed to the motion of sawdust. Elsewhere, Ahmad and Alsaedi (2009) conducted a study, which developed a generalized quasilinearisation technique for a sequence of approximate solutions converging monotonically and quadratically to the unique solution of the forced Duffing equation, with discontinuous type integral boundary conditions. However, information concerning application of this model in the real life case studies of sawmills is missing in the work. Yet in another study, Ahmad and Aighamdi (2008) studied a boundary value involving the non-linear Duffing equation. Ahmad et al. (2008) further extended the frontier of knowledge by considering Duffing equations with integral bounding conditions. However, neither of these studies discussed any practical issues relating to the motion of sawdust. In a study by Zhang and Xiang (2007), discussion centred on a Duffing oscillator algorithm based on the Duffing system such that signal-to-noise ratio was improved. The practical application of the work did not extend to the case of sawdust, thus creating a research gap which this work attempts to fill.

The work of Salau and Oke (2010) addresses sawmill activities and is in this respect similar to the present work. However, this work is limited in that extensive statistical analysis using a variety of statistical approaches is required for the validation of the work. Other studies on sawdust include those of Hamdaoui (2006), Šæiban et al. (2006), Hamadi et al. (2001), Jadhav and Vanjara (2004), and Taty-costodes et al. (2003). These authors considered the economics of sawdust in terms of sorbent and absorbent materials. The aspect considered by Akira et al. (2002), Ansari and Raofie (2006) are the utilization of sawdust for boiler processes as well as catalytic actions, respectively. These studies on sawmill did not consider sawdust motion apart from that of Salau and Oke (2010). It seems reasonable to conclude that to the best of the authors' knowledge, the extensive literature on emission, sawdust and Duffing equations have not solved the problem of dynamic system time series prediction using 2D-graphical means.

Sawmill operations management is cost intensive in nature and need proper cost control to enhance high profit margin for the sawmill business. The requirement of governments in terms of high penalty cost, accident and compensation costs have therefore prompted the need to capture data for proper control of health problems in sawmills through sawdust movement modelling, data collection and analysis. However, the traditional approach of obtaining information through time history is costly in view of the dynamic nature of the particle formation system of sawdust in sawmills soon after dispersion from the band saws.

UNIVERSITY OF IBADAN LIBRARY

Though alternatives to Duffing's equation can be used to undertake the same analysis proposed in this work, alternative equations and methods are not as robust as the current work. They are weak in capacity to handle non-linear phenomena and could only treat singular analysis. However, the choice of Duffing's equation among others is guided by the fact that it is very rich in exhibiting non-linear phenomena and also can combine several parameters. It exhibits chaotic behaviour and poincare section which makes some parameter combinations to produce unusual fractal configurations. Equally, sawdust dynamics are expected to exhibit a range of these non-linear phenomena. The objective of this study is to device a transformation system in 2-dimensional Euclidean space that will enable a 2-dimensional graphical representation of dynamic sawdust particle motion compared to the high cost alternative of time series configuration. The purpose is for the long time prediction of sawdust motion after emission from the band saw during the cutting action.

3.0 MODEL EQUATIONS AND METHOD

The models used for this study included harmonic functions of unity amplitude, the model of Duffing's dynamical system and the linear transformation model. Duffing's model has its basic foundation in the classic study of Baker and Gollub (1990) as well as the work of Gleick (1987), and offers a new contribution when applied to the problem of sawdust particle motion in sawmill environments. In modelling the motion of sawdust particles in the sawmill environment, the particle is visualized as randomly floating in the air, in order to capture all the features of the anticipated transformed time series. In order to move in the different directions (x, y, or z), the sawdust particle needs to overcome resistance against movement in the air. The drag forces and frictional forces act separately but simultaneously on particles moving in a fluid, to slow down or resist their movement. The two forces are predicated on the shape and surface of the particle, respectively.

The sawdust particle, as soon as it is produced from the interaction of the cutting edge of the band saw with the wood piece, is driven non-linearly about by the combined effect of the force of gravity, wind forces, emission forces, its geometry, and air properties. Other factors that impinge on the movement of the sawdust particle include; efficiency of the sawmill operation that is dependent on its age, humidity, temperature, as well as particle size and density. These factors were assumed constant in view of limited resource constraints to actualise their measurements. The wind velocity is an important factor that influences the direction of motion of the sawdust particle by tending to carry the particle in its direction of propulsion. However, in view of the prohibitive costs of acquiring equipment for measuring wind speed, humidity and temperature and that of collecting relevant practical data, these parameters were assumed have no dynamic effect on the sawmill cutting operations; the operator was assumed to work under normal atmospheric conditions of temperature (room air temperature, 37^0C). The efficiency of the sawmill operator was assumed to be of a standard acceptable in practice. Although, ignoring these factors has implications on the accuracy of the predictions arising from the present work, the study provides a basis for further investigations in a research area where scanty information is available. If accurate figures of wind speed and velocity over the years for dry, rainy and harmmatan seasons were available, then relationships between wind speeds, sawdust particle speed after emission and the quantity of sawdust produced for different species of wood could be established and used to estimate the minimum and maximum quantities of sawdust inhalable by the sawdust operator. Information from this could help government legislation that no operator should spend beyond certain years doing the same work in the sawmill environment so as to safeguard the health of workers.

The simplified model developed for this scenario visualized the sawdust motion as described by Duffing's equation with the numerical solution acting as a transformation scheme.

The development of a theoretical model in this work starts with two familiar harmonic functions given here as Equations 1a and 1b, thus:

$$F(t) = \text{Cos}(\omega t) \quad (1a)$$

$$F(t) = \text{Sin}(\omega t) \quad (1b)$$

Where $F(t)$ = time series, ω = frequency measured in radians per second, and t = time in seconds. The product ωt is measured in radians.

The mathematical model for Duffing's dynamic system is generally written as shown in Equation 2. However, the form used in this study is as shown in Equation 3 since it is a particular case of Equation 2, which has been used in the literature to predict the dynamics of particle motion [Moon (1987); Dowell (1988); Baker and Gollub (1990)]. Application of Equation 3 using a sawmill as a case study and in particular, studying sawdust dynamics helps to further establish the utility of Equation 3 in the present work. It is well known that this form of Duffing's equation (i.e. Equation 3) can exhibit chaotic solutions (under some combinations of displacement and velocity parameters) apart from the fixed and periodic behaviour that it also exhibits. The property of the chaotic solutions exhibited by Equation 3 is rarely obtained from the general Equation 2. It is

UNIVERSITY OF IBADAN LIBRARY

 © KJME 2010

anticipated, as shown in Moon (1987), Dowell (1988) and Baker and Gollub (1990), that the worst dynamics of sawdust particles will be chaotic for some driving parameters.

$$\ddot{x} + \gamma\dot{x} - x(1 \pm 0.5x^2) = P_0 Cos(\omega t) \quad (2)$$

$$\ddot{x} + \gamma\dot{x} - x(1 - 0.5x^2) = P_0 Cos(\omega t) \quad (3)$$

Where, x = displacement; $\dot{x}$ = velocity; γ = damping coefficient; P_o = forcing amplitude; ω = forcing frequency and t = time into the future.

Equation 3 can be written as a pair of first order differential equations by letting:

$x_1 = x$ (displacement) (4a)

$x_2 = \dot{x}$ (velocity) (4b)

Differentiating Equations 4a and 4b once with respect to time gives rise to:

$$\dot{x}_1 = x_2 \quad (5a)$$

$$\dot{x}_2 = -\gamma x_2 + x_1(1 - 0.5x_1^2) + P_0 Cos(\omega t) \quad (5b)$$

Numerical solutions for Equation 5b were sought here using programs written in Fortran, for arbitrarily selected parameters and initial conditions. The parameters selected were arbitrarily chosen as this demonstrated the flexibility with which the Fortran program used as the source codes accepted input parameters for the intended simulation. Equations 5a and 5b were solved simultaneously using a Runge-Kutta based algorithm to guarantee a reliable numerical solution.

The corresponding solutions obtained were transformed linearly in accordance with the transformation given in Equation 6, and the arising components computed as shown in Equations 7a and 7b.

$$(\text{Time SeriesValue})_{New} = (\text{Time SeriesValue})_{Old} + (\text{Minimum Time SeriesValue})_{Old} \quad (6)$$

The time series values are solutions to the function, $F(t)$, in Equations 1 and 2, and solutions to displacement and velocity in Equations 5a and 5b.

Let the Radius (R) be equal to the $(\text{Time Series Value})_{New}$, and the New time measured in radians be designated by the symbol, θ, where θ is also equal to the Modulated Old Time. The x and y-coordinate components of R can be obtained using Equations 7a and 7b, respectively, thus:

X-component = RCos(θ) (7a)

Y-component = RSin(θ) (7b)

4.0 RESULTS AND DISCUSSION

4.1 Simulation Results

The results of this study are presented graphically in the form of time graphs, phase plots and 2-D time series representations of Duffing's dynamic system. The figures presented are for different parameters and specified initial conditions. The main reason for the selection of different parameters for the figures is because chaotic systems are highly sensitive to the driving parameters, especially the initial conditions. Thus, it becomes essential to link graphical results to the driving parameters used for their generation.

UNIVERSITY OF IBADAN LIBRARY

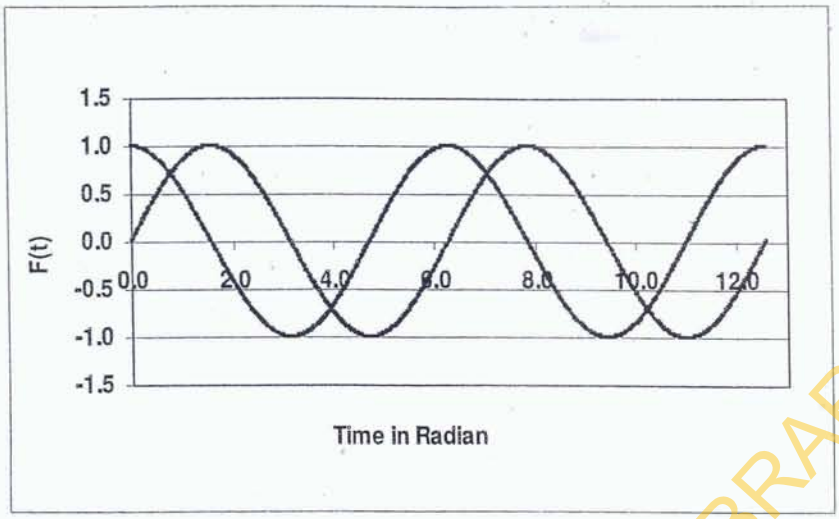

Figure 1 **2-Cycles Graphical Representation of the Time Series Functions, $F(t) = \text{Cos}(\omega t)$ & $\text{Sin}(\omega t)$, for $\omega = 1.0$ *rads/sec***

Figure 1 represents a two cycle solution of the functions, $F(t) = \text{Cos}(\omega t)$ & $\text{Sin}(\omega t)$, with 1001 solution points per cycle and $\omega = 1.0$ rads/sec. The pattern in Figure 1 repeats itself ad-infinitum as both $\text{Cos}(\omega t)$, which appears in blue and $\text{Sin}(\omega t)$, which appears in purple, are periodic in time. The two dimensional representation of these functions are explored further in subsequent figures for $\omega = 1$ and 0.5 rads/sec, respectively.

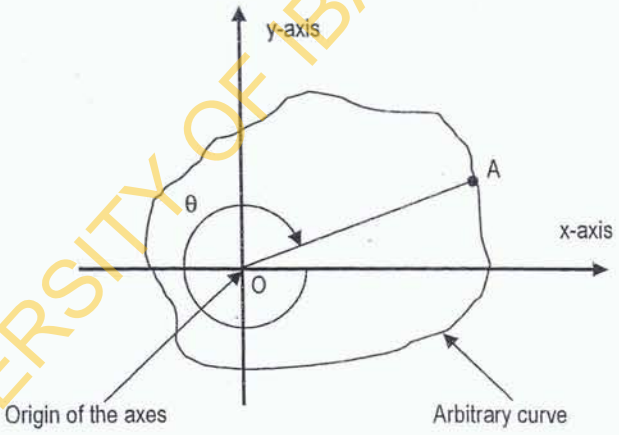

Figure 2 An Arbitrarily Closed Curve

Figure 2 and the ensuing paragraph explain how the minimum values are read from the corresponding graphs of Figures 3 to 14. For the arbitrary closed curve shown in Figure 2, The length, *OA*, in Figure 2 designates a radius originating from the point, *O*, which is the origin of the *x* and *y* axes. The radius, *OA*, cuts the arbitrary closed curve at location *A*. An arbitrary closed curved is used since it has features of the anticipated transformed time series. The direction of the radius is given by the angle, θ, measured from the *x*-axis and turning in a clockwise direction. The origin in this illustration is the source of the emitted sawdust at the point of contact between the wood and the band saw, from where sawdust is produced, which then moves in continuous motion, starting from the time that the timber is loaded on the cutting table and pushed through the cutting blade. The radius, *OA*, indicates the maximum distance of the respective sawdust particles from the band saw, and can be similarly defined for other known radii and angles. The reading of the minimum value of the respective sawdust particles from the band saw was inbuilt in the Fortran program given in the appendix, using the highlighted statements in the source codes.

UNIVERSITY OF IBADAN LIBRARY

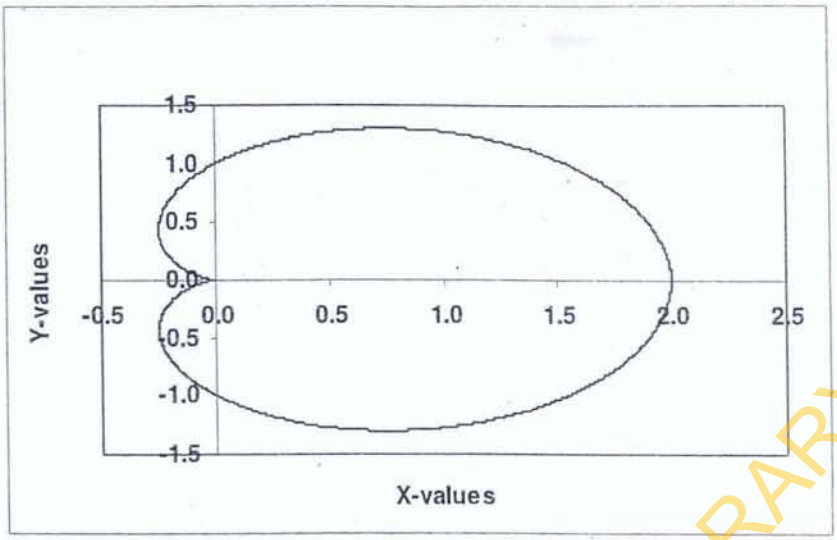

Figure 3 2-D Representation of Time Series $F(t) = \text{Cos}(\omega t)$ for $\omega = 1.0$ *rads/sec*, and $F_{min} = -1.0$

Figure 3 represents the two period solution of the function, $F(t) = \text{Cos}(\omega t)$, with 1001 solution points per period and $\omega = 1.0$. In Figure 2, a single closed loop is observed resident in the finite plane area as evidence of the periodicity of the function, $F(t) = \text{Cos}(t)$. The radii from the origin of the axes cut the closed loop once at any angle measured with reference to the positive *x*-axis and turning clockwise. Figure 2 can be used to predict the $F(t)$ value of the respective sawdust particles by adding the corresponding radius to the recorded F_{min} value of the same. F_{min} has the same meaning as the $(\text{Minimum Time Series Value})_{old}$ in Equation 6. It gives the value of the minimum recorded steady solution of the sawdust particle in motion obtained from the trigonometric functions (i.e. sin and cos) or Duffing's equation

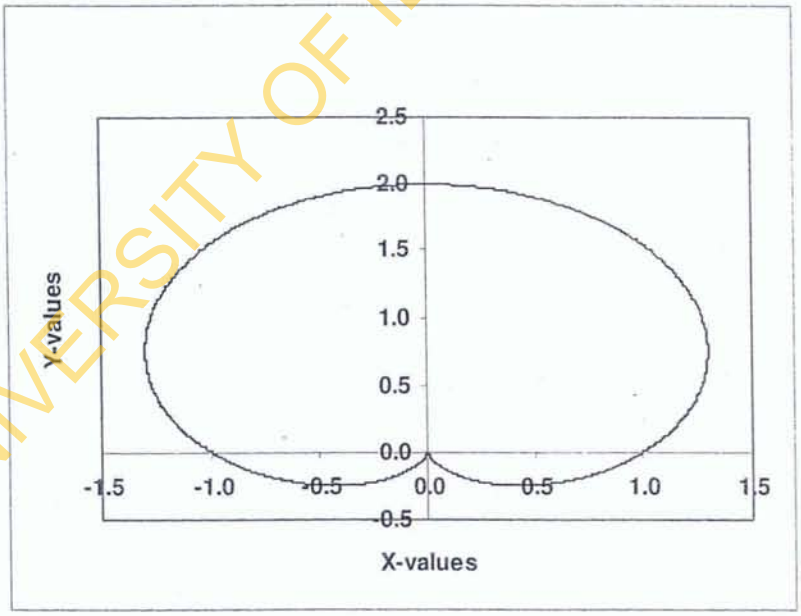

Figure 4 2-D Representation of Time Series $F(t) = \text{Sin}(\omega t)$, for $\omega = 1.0$ *rads/sec*, and $F_{min} = -1.0$

Figure 4 represented the two period solution of the function, $F(t) = \text{Sin}(\omega t)$, with 1001 solution points per period and $\omega = 1.0$ rads/sec. In Figure 3, a single closed loop is observed resident in the finite plane area as evidence of the periodicity of the function, $F(t) = \text{Sin}(\omega t)$. The radii from the origin of the axes cut the closed loop once at any angle measured with reference to the positive *x*-axis and turning clockwise. Figure 3 can be used to predict the $F(t)$ value of the respective sawdust particles by adding the corresponding radius to the recorded F_{min} value of the same.

UNIVERSITY OF IBADAN LIBRARY

 © KJME 2010

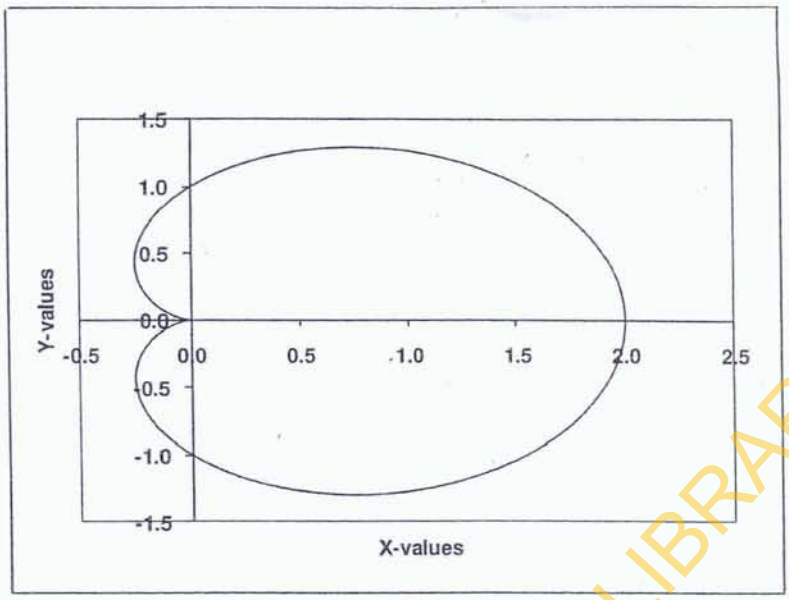

Figure 5 2-D Representation of Time Series $F(t) = \text{Cos}(\omega t)$, for $\omega = 0.5$ *rads/sec*, and $F_{min} = -1.0$

Figure 5 represents the two periods solution of the function, $F(t) = \text{Cos}(\omega t)$, representing the motion of the sawdust particle after emission from the band saw, with 1001 solution points per period and $\omega = 0.5$. In Figure 5 a single closed loop is observed resident in the finite plane area as evidence of the periodicity of the function, $F(t) = \text{Cos}(0.5t)$. The radii from the origin of the axes cut the closed loop once at any angle measured with reference to the positive *x*-axis and turning clockwise. Figure 5 can be used to predict the $F(t)$ value of the respective sawdust particles by adding the corresponding radius to the recorded F_{min} value of the same.

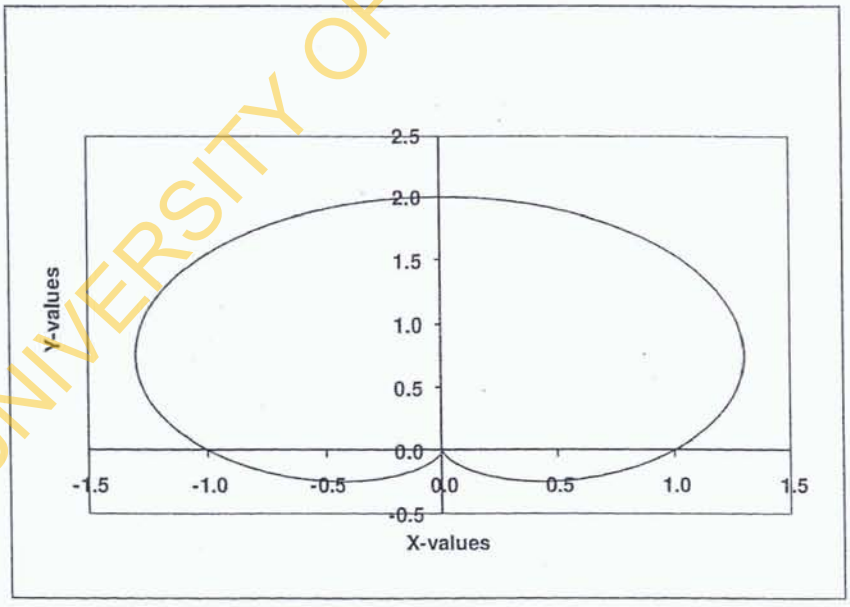

Figure 6 2-D Representation of Time Series $F(t) = \text{Sin}(\omega t)$, for $\omega = 0.5$ *rads/sec*, and $F_{min} = -1.0$

Figure 6 represents the two periods solution of the function, $F(t) = \text{Sin}(\omega t)$, which describes the motion of the sawdust particle, with 1001 solution points per period and $\omega = 0.5$ rads/sec. In Figure 6 a single closed loop is observed resident in the finite plane area as evidence of periodicity of the function, $F(t) = \text{Sin}(0.5t)$. The radii from the origin of the axes cut the closed loop once at any angle measured with reference to the positive *x*-axis and turning clockwise. Figure 6 can be used to

UNIVERSITY OF IBADAN LIBRARY

predict the F(*t*) value of the respective sawdust particles by adding the corresponding radius to the recorded F_{min} value of the same. The results presented in Figures 3 to 6 form the basis for the corresponding analysis of the periodic and chaotic function, F(*t*), found in Duffing's dynamic system modelled by Equation 5.

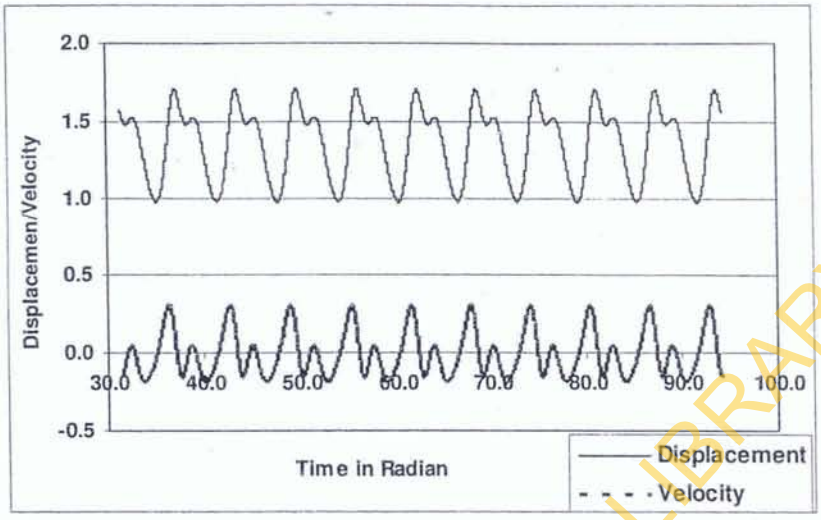

Figure 7 Duffing's Time Graph (Damping = 0.4 *Ns/m*, Excitation Force = 0.4*N* and ω = 0.5 *rads/sec*)

Figure 7 represents a ten (10) forcing period solution of Duffing's dynamic system with 1001 solution points per period. The initial displacement and velocity of the sawdust particles were 2*m* and 1 ms^{-1} respectively. The first five periods of the solution were discarded to guarantee a stable solution through instructions that were coded in the Fortran program source codes developed here. The first five solutions were regarded as transient solutions and were and discarded. This assumption was validated by the good comparison observed between the results generated by software developed here and those obtained from literature.

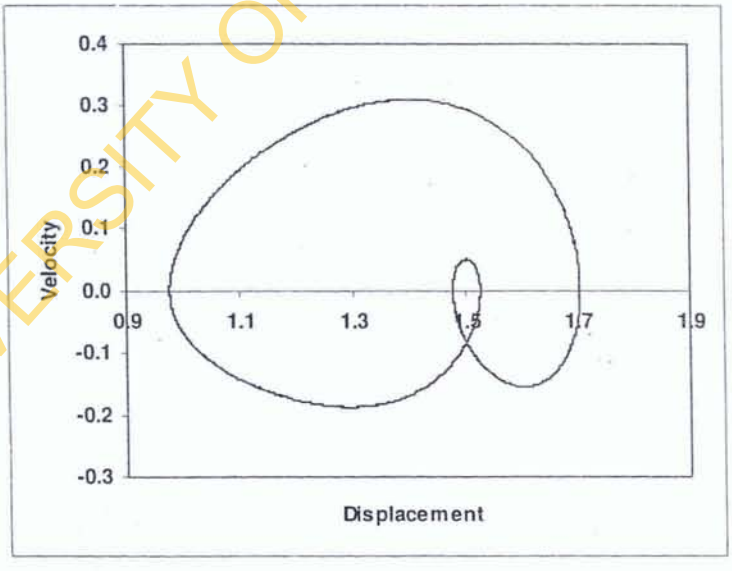

Figure 8 Phase Plot for Duffing's (Damping =0.4 *Ns/m*, Excitation Force = 0.4*N* and ω = 0.5 *rads/sec*)

Figure 8 presents the same information contained in Figure 7, but this time in the form of a phase plot. Phase plots enable a compact presentation of information that can extend to infinity along the time axis in time graphs such as the one shown in Figure 7, in finite 2-D Euclidean dimensions.

UNIVERSITY OF IBADAN LIBRARY

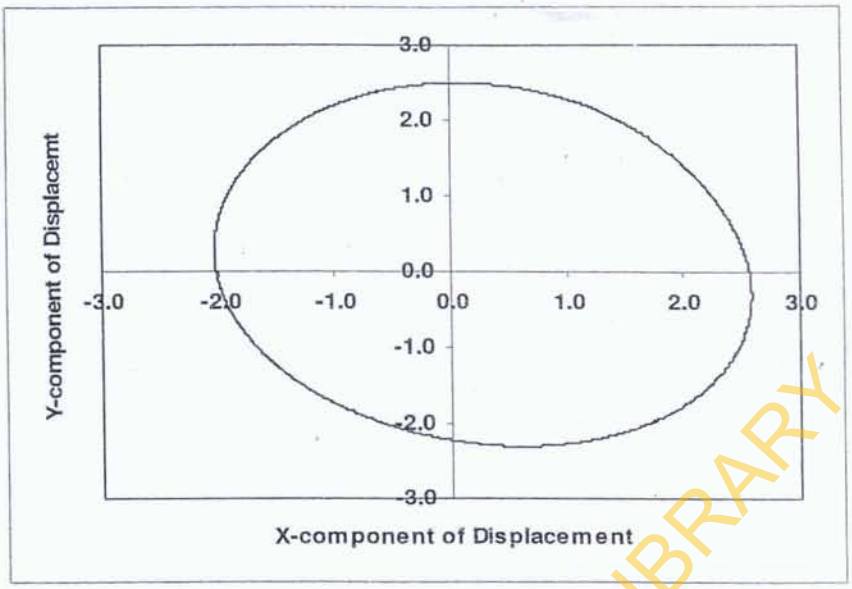

Figure 9 2-D Representation of Displacement of Duffing's (Damping =0.4 *Ns/m*, Excitation Force = 0.4*N* and ω = 0.5 *rads/sec*)

Figure 9 presents the same information presented in Figure 7 for displacement but this time in the form of a 2-dimensional plot. The time axis in Figure 9 is compressed and has the same dynamic interpretation as the phase plot shown in Figure 8. The displacement values of the respective sawdust particles in Figure 9 repeat themselves at regular time intervals of 2π. In addition, the time (in radians) for the displacement components can be read from this 2-D representation using the positive *x*-axis as a datum and turning clockwise. Figure 9 can be used to predict **Duffing's displacement** value of the respective sawdust particles by adding the corresponding radius to the recorded minimum displacement of **-0.9757*m***. This value **-0.9757*m*** cannot be read from the graph in Figure 9 though and is obtained from the steady solutions of Duffing's equation presented in the program in Appendix-II. This minimum value of the respective sawdust particles was determined using the five bolded statements in the program shown in this appendix. The write on screen statement in this program enabled the computer to display the value thus determined on the computer screen from where it was then picked.

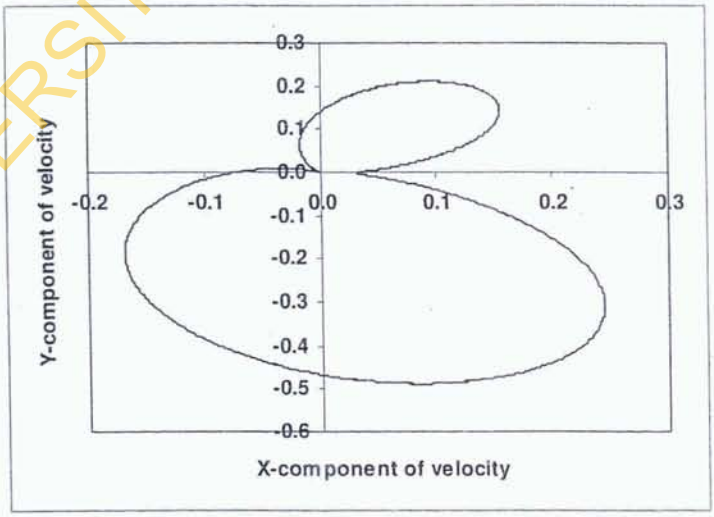

Figure 10 2-D Representation of Velocity of Duffing's (Damping =0.4 *Ns/m*, Excitation Force =0.4*N* and ω = 0.5 *rads/sec*)

UNIVERSITY OF IBADAN LIBRARY

© KJME 2010

Figure 10 presents the same information shown in Figure 7 for velocity but this time in the form of a 2-dimensional plot. The time axis in Figure 10 is compressed and has the same dynamic interpretation as the phase plot shown in Figure 8. The velocity values repeat themselves at regular time intervals of 2π. In addition, the time (in radians) for the velocity components can be read from this 2-D representation using the positive x-axis as a datum and turning clockwise. Figure 10 can be used to predict **Duffing's velocity** value of the respective sawdust particles by adding the corresponding radius to the recorded minimum velocity **-0.1878 ms^{-1}.** The value -0.1878 ms^{-1} was similarly obtained as the recorded minimum displacement value of -0.9757m, discussed in the preceding paragraph.

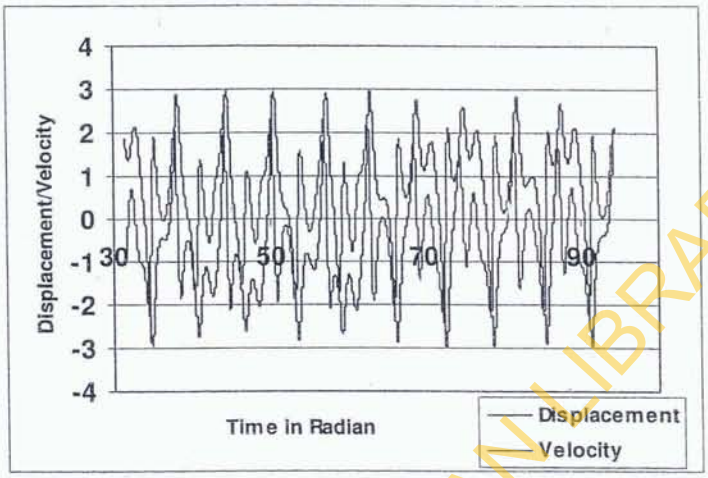

Figure 11 **Duffing's Time Graph (Damping =0.4 *Ns/m*, Excitation Force =2.1*N* and ω = 0.5 *rads/sec*)**

Figure 11 presents a ten (10) forcing period solution of Duffing's dynamic system with 1001 solution points per period and ω = 0.5. The initial displacement and velocity of the sawdust particles are 2m and 1 ms^{-1} respectively. The first five (5) periods of the solution were discarded to guarantee a stable solution, and are not included in Figure 11.

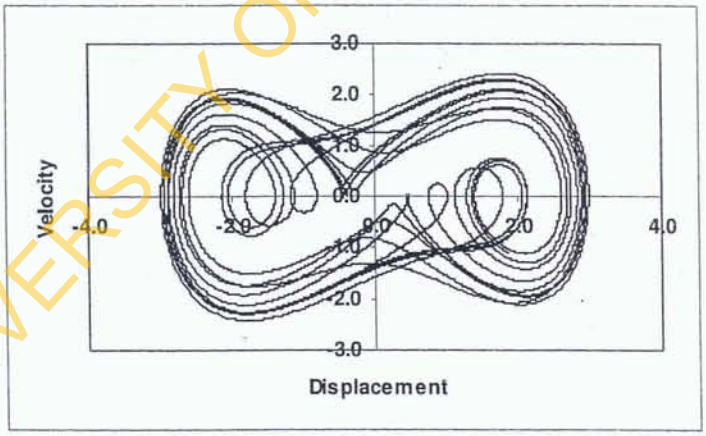

Figure 12 **Phase Plot for Duffing's (Damping =0.4 *Ns/m*, Excitation Force =2.1*N* and ω = 0.5 *rads/sec*)**

Figure 12 presents the same information contained in Figure 11, but this time in the form of a phase plot. The advantages of phase plots over time graphs have already been mentioned here. The multiple loops shown on in Figure 12 are evidence of the chaotic dynamics of Duffing's equation [Gleick (1987); Baker and Gollub (1990)]. The loops cut any selected radii in more than one place, which is evidence of the multiple solutions probing the system in time.

UNIVERSITY OF IBADAN LIBRARY

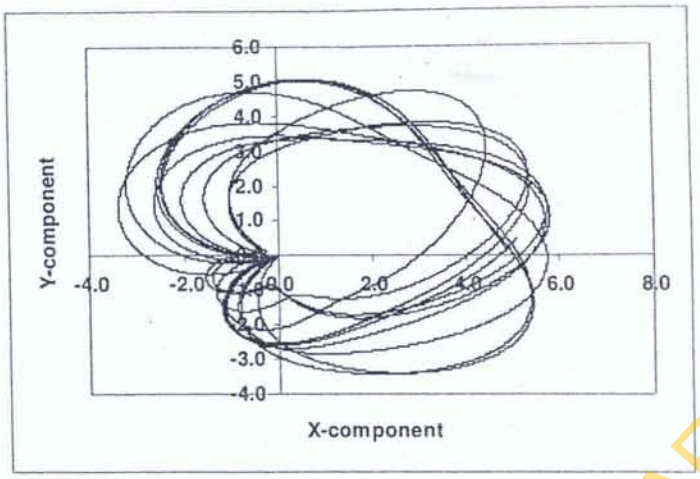

Figure 13: 2-D Representation of Displacement of Duffing's (Damping =0.4 *Ns/m*, Forcing =2.1*N* and ω = 0.5 *rads/sec*)

Figure 13 presents the same information shown in Figure 11 for displacement but this time in the form of a 2-dimensional plot. The time axis in Figure 13, which is perpendicular to the plane containing the *x* and *y* components, is compressed and has the same dynamic interpretation as the phase plot in Figure 12. The displacement value is irregular over a time interval of 2π. In addition, the time (in radians) for the displacement components can be read from this 2-D representation using the positive *x*-axis as a datum and turning clockwise. Figure 13 can be used to predict **Duffing's displacement** value by adding the corresponding radius to the recorded minimum displacement of **-2.9913*m***.

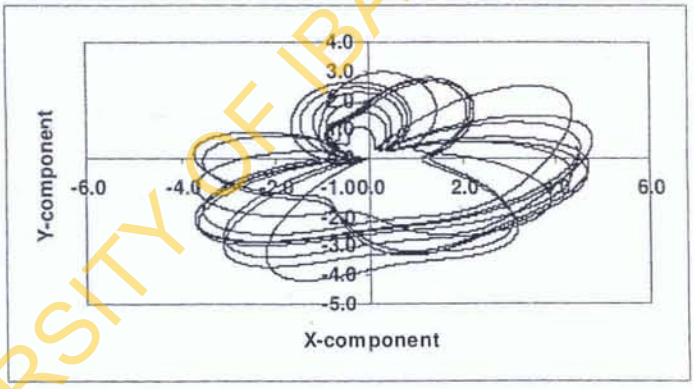

Figure 14 2-D Representation of Velocity of Duffing's (Damping =0.4 *Ns/m*, Excitation Force =2.1*N* and ω = 0.5 *rads/sec*)

Figure 14 presented the same information presented in Figure 11 for velocity but this time in form of a 2-dimensional plot. The time axis in Figure 14, which is perpendicular to the plane containing the *x* and *y* components, is compressed and has the same dynamic interpretation as the phase plot in Figure 12. The velocity value is irregular over a time interval of 2π. In addition, the time (in radians) for the displacement components can be read from this 2-D representation using the positive *x*-axis as a datum and turning clockwise. From Figure 14, the Duffing's velocity value of the respective sawdust particles can be predicted by adding the corresponding radius to the recorded minimum velocity of -2.4238 ms^{-1}.

4.2 Field Experimental Results

A field experiment was carried out in a local sawmill located in Lagos, Nigeria, to determine the important attributes of sawdust particles relevant to this study and the sawmill characteristics with which real practical information could be

UNIVERSITY OF IBADAN LIBRARY

compared with the theoretical simulated characteristics of the sawdust particles. The prominent information gathered relates to the displacement of the sawdust particles away from the source of emission (the contact point of the blade with the wood loaded on the machine for cutting) and well as the time it takes to hit a board positioned at designated points. The dimensions of the sawdust particles were observed on a mass spectrometer (Table 1). The measurement of the displacement of the sawdust particles was in meters and was measured relative to the angle of inclination that the particles made with the centre point of the cutting blade on the machine. Time of motion of sawdust particle was measured in seconds while the dimensions of the sawdust were measured in millimetres. From the two sets of data on displacement and time, computation of the velocity of travel of sawdust particles away from the point of contact of machine/cutting blade and the logs being fed to the machine was made in meters per second. For the workshop visited, data was collected from two machines. One of the cutting machines from which data was collected was used for smoothening the planks while the other one was used for cutting the planks into various shapes. The data collected was then grouped into two (Table 2 and 3). Each of the machining processes produced different forms of sawdust, which varied in sizes, weights and appearances. The scrapping process produced coarse or hard sawdust (Table 2), which needed further processing for the production of finer sawdust (Table 3). The two machines were separated by a distance of 45 inches and each had a width of approximately 25 inches. For each sets of time estimation, using the stopwatch, time measurements were made with the average computed, indicating the mean while the standard deviation of the sets of data were also computed.

Table 1 Length and Breadth of Sawdust Particles Obtained from Sampling

S/N	Length (*mm*)	Breadth (*mm*)
1	0.006	0.006
2	0.004	0.002
3	0.004	0.003
4	0.005	0.003
5	0.006	0.007
6	0.001	0.001
7	0.005	0.002
8	0.006	0.005
9	0.005	0.005
10	0.002	0.005

Table 2 Data on Displacement and Timeframe for the Coarse Grains (by Smoothening) Sawdust Obtained During the Cutting Operation

S/N	Displacement (*m*)	Time (*s*)	Angular position of analyst to the tip of the blade (degrees)	Velocity (*m/s*)
1	1.03	4.05	35	0.2543
2	1.43	4.60	30	0.3109
3	1.84	3.45	180	0.5333
4	3.27	4.85	180	0.6742
5	4.10	5.50	180	0.7454

Table 3 Data on Displacement and Timeframe for the Fine Grains Sawdust Obtained During the Cutting Operation

S/N	Displacement (*m*)	Time (*s*)	Angular position of analyst to the tip of the blade (degrees)	Velocity (*m/s*)
1	0.37	1.89	45	0.1958
2	0.37	2.01	60	0.1762
3	0.47	2.13	180	0.2207

By establishing linear functions for the relationships between velocity and displacement for the fine grain sawdust, and also for the relationships between velocity and time for each of the fine grain and coarse grain sawdust, the equations arising (shown below) serve well for making predictions.

UNIVERSITY OF IBADAN LIBRARY

 © KJME 2010

$V_1 = 5.906 - 14.154D_1$ (velocity and displacement, fine grain) (8)
$V_2 = 2.4303 - 0.8255D_2$ (velocity and displacement, coarse grain) (9)
$V_3 = 3.0362 - 1.3915D_3$ (velocity and time, fine grain) (10)
$V_4 = 4.8781 - 0.9743D_4$ (velocity and time, coarse grain) (11)

Where V_1, V_2, V_3 and V_4 are velocities while D_1, D_2, D_3 and D_4 displacement quantities.

Comparative analysis was done between the values obtained from field studies and the theoretical values obtained using graphs presented here earlier, with the result that the simulations arising from the present work were seen to rightly mimic reality.

5.0 COMPARISON AND ANALYSIS OF THE RESULTS AND THEIR APPLICATION

5.1 Analysis of the Results

The results shown in the preceding section validate the real life model. The last part of section 3 shows the results obtained from field study of practically observed sawdust particles in motion. The data is pilot as it is small and more extensive data is required in order to develop a better understanding of the behaviour of sawdust particles. However, data collection in the sawmill industry is potentially risky and care should be taken when collecting more extensive data for further validation of the work presented here. To provide further insights into the connection of these results to sawdust movement, the phase plane plot of Figure 11 is explained using control theory, with reference being made to the chaotic oscillation of mechanical systems, as reported by Dowell (1988). The factor, K, is an indicator of control strength as argued in the paper. For the values of K outside the range 0 to 3.999, the solution of logistic model Equation 3 will grow without bounds and this is totally unwanted in the current study. Rather, it is desire that the solution bounces around and within definite limits. Specifically, the solution should be bounded between a minimum value of zero and a maximum value of 1.0. The distribution of the solution can confirm fixed, periodic or chaotic behaviour, but never random behaviour. The chaotic solution is what the present study utilise to drive the particle marked A' in the Euclidean space. For the same reason, Lyapunov tool was employed to reveal a pass or fail test for the solution generated for specified K-values. A pass implies that the solutions obtained at the specified K-value is chaotic, and a fail otherwise. The constant step of 0.001 is to ensure thorough check for all K-values between the 0 and 3.999 limits that lead to chaotic solution.

Now, referring to the preceding paragraph, the choice of directions for the solution described therein are developed as follows for 1-D, 2-D and 3-D Euclidean Spaces. For 1-D Euclidean Space, the description is as follows:

(1) Move a step (size picked randomly from 0 to 1.0) to the right if solution is $0 \leq s \leq 0.5$
(2) Move a step (size picked randomly from 0 to 1.0) to the left if solution is $0.5 \leq s \leq 1.0$

Considering 2-D Euclidean Space, the following steps may be helpful:

(1) Move a step (size picked randomly from 0 to 1.0) to the North if solution is $0 \leq s \leq 0.25$
(2) Move a step (size picked randomly from 0 to 1.0) to the South if solution is $0.25 \leq s \leq 0.5$
(3) Move a step (size picked randomly from 0 to 1.0) to the East if solution is $0.5 \leq s \leq 0.75$
(4) Move a step (size picked randomly from 0 to 1.0) to the West if solution is $0.75 \leq s \leq 1.0$

However, for 3-D Euclidean Space, the following steps are needed:

(1) Move a step (size picked randomly from 0 to 1.0) to the North if solution is $0 \leq s \leq 0.167$
(2) Move a step (size picked randomly from 0 to 1.0) to the South if solution is $0.167 \leq s \leq 0.334$
(3) Move a step (size picked randomly from 0 to 1.0) to the East if solution is $0.334 \leq s \leq 0.501$
(4) Move a step (size picked randomly from 0 to 1.0) to the West if solution is $0.501 \leq s \leq 0.608$
(5) Move a step (size picked randomly from 0 to 1.0) to the Toward Roof if solution is $0.608 \leq s \leq 0.775$
(6) Move a step (size picked randomly from 0 to 1.0) to the Toward Floor if solution is $0.775 \leq s \leq 1.0$

Where the symbol, s, above is the same as the sequence of chaotic solutions (X_n) obtained by solving Equation 3 in this paper.

The step size can be a fixed value (i.e. 1.0) or picked randomly between 0 and 1.0 as explained above. The corresponding β values obtained from invoking Equation 8 on particle A' for all K-values that lead to chaotic solutions are contained in Figures 5, 6 and 7. Figure 5 is the results obtained for particle A' in 1-D Euclidean space, Figure 6, the results obtained for particle A' in 2-D Euclidean space, and Figure 7 is the results obtained for particle A' in 3-D Euclidean space. The practical

 © KJME 2010

UNIVERSITY OF IBADAN LIBRARY

value of for low and high values of parameter, β, is that high values of β signify fast diffusion in the studied space and vice versa for the lower values of β.

The phase plots presented in this work indicate that for the applied driving parameters, the sawdust particles are unable to settle down to any static equilibrium positions after their emission from the band saw of the cutting machine. Instead, the sawdust particles are circulated in a competitive manner. The word competitive here refers to the various directions in which the sawdust particles may move. The sawdust particles may move to the north, south, east, west, up and down or in combinations of any of these six directions under the influence of the driving parameters of; wind forces, particle density, shape, and humidity. Since no information was available literature with respect to the driving parameters, they were not considered here and further scientific work would be required in order to incorporate them into the models developed in this work. Using Figure 15 as a reference, the equilibrium positions of a sawdust particle may be given by the position vectors, (-√2, 0); (0, 0) and (+√2, 0), referred to Equations 5a and 5b, using equilibrium analysis. In this figure, the spring behaves non-linearly while the damper behaves linearly as captured by Equations 5a and 5b.

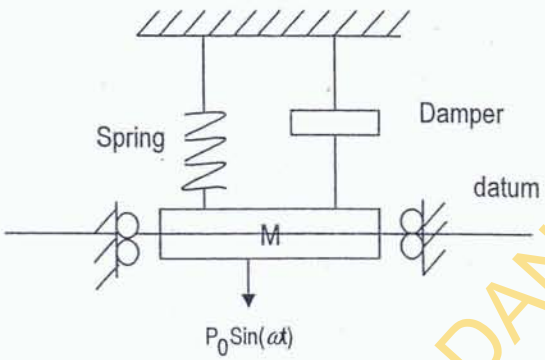

Figure 15 A Schematic of Duffing's Oscillator Representing Sawdust Particle Behaviour

The object of interest is the mass, *M*, representing a sawdust particle under the action of the external force, $P_0\text{Sin}(\omega t)$, spring and damper). In the absence of external forces, the centre of the mass *M* can choose to settle down along the line marked as datum, below or above it, representing three static equilibrium positions, given above as; (-√2, 0), (0, 0), and (+√2, 0). Now, applying the principle of the Duffing's oscillator to a sawdust particle in its motion along the line marked as datum, below or above it as in the sawmill environment, the constraint of being limited to up and down movements is removed since the sawdust particle would be freely suspended in air and not rigidly fixed to a body. This is the real behaviour of sawdust particles in the sawmill, as the sawdust particle is free to move in all chosen directions. However, its relocation stepping can vary widely as time passes in constant step units. The sawdust particle has the freedom to choose between the range of shortest, longest and possible lengths in between these two extremities. This varying stepping represents the time history of the sawdust particle. These three static equilibrium positions could be confirmed by setting $\dot{x}_1 = \dot{x}_2 = P_o = 0$ and then solving for the pair of (x_1, x_2) that satisfy the resulting equations. Furthermore, an important aspect of the present work is the inbuilt Fortran and Excel programs which serve as source codes that enable the solution of Duffing's equation and which can quickly do the transformation stated in Equation 6. This is done before plotting the graphs for visual appreciation.

This work has presented results of the various scenarios, representing the mathematical behaviour of the models. These correspond to the sawdust particle movement in the sawmill environment. In the graphs presented for the current work, there is usually a reference point, 0, which is referred to as the origin, as well as the negative and positive *x* and *y* points. This point, 0, for the graphs indicate the contact point of the band saw blade with the wood piece. As soon as the sawdust is produced, it is blown by the air in an upper direction and then deflected to the left or right. The degree of deflection depends on the magnitude of the velocities imparted on the particles on exit from the bands saw/wood point of contact. It is from the foregoing understandable that the various shapes presented in Figures 3 to 14 in this work are a reflection of the guiding Equations 1 to 7. The current study is verified by Bello and Mijinyawa (2010) who reported on–site observations on heaps of wood shavings from planning machines and sawdust accumulation around circular and band saws. The study by Srinivasakannan and Subramanian (2008) is also a validation of the information provided above on the movement of sawdust through the reported investigation on the drying kinetics of sawdust in tray dryer.

UNIVERSITY OF IBADAN LIBRARY

© KJME 2010

5.2 Comparison of the Results

The current paper is a follow-up of another paper on the subject of modelling of the motion of sawdust. A comparative analysis of these two papers (the present one and the one by Salau and Oke, 2010) highlights both similarities and differences. The computational time for the transient as well as steady solutions is very high in both papers, which are about two minutes for the current paper and 5 minutes for the paper by Salau and Oke (2010) using Pentium M computer in both cases. The term "very high" means long transient and steady solution periods. It is known that seeking a numerical solution is a stepwise process. For dynamic systems the first set of solutions are usually regarded as unstable and there is no theoretical means of determining when (i.e. in how many steps) the solution transits to stability. The available practical means is to wait for a long computation time as a stable solution serves a good basis for conducting numerical studies. Very high period (say between 2 and 5 minutes) is similarly defined and requires a long time for a stable solution period to emerge. The transformation of time series (time value as *x*-axis and series value as *y*-axis) is to 2-dimensional Euclidean spaces (series value as *x*-axis and series values as *y*- axis) in both papers. Similarly, aggregation of sawdust particles was studied in the 2-dimensional Euclidean space, thus making the 2-dimension Euclidean space a common factor in both papers. Cost reduction due to the time saved modelling in comparison to time taken to collect actual physical data was also common to the other paper. This paper attempted to summarise several pages of time series sawdust particles trajectory information on a set of single phase plots of the dynamic system modelled. The work of Salau and Oke (2010) was similar in some way to the current work in that it aimed at reducing health service cost. While Salau and Oke (2010) utilised fractal aggregation of sawdust particles, the current paper presents an understanding of the subject of particle movement based on chaotic walk principles. In addition, the two papers aimed at addressing problems associated with uncontrolled sawdust in motion in the sawmill industry. Further, the two papers present numerical models aimed at describing the behaviour of particles, with the expectation that this behaviour can be used to describe observed phenomena of sawdust that is generated in sawmill industries. Collection of practical data from the field is therefore necessary to validate the models developed in both papers.

While the current paper focuses on the transformation of sawdust particles trajectory (tagged time series), the emphasis of the paper by Salau and Oke (2010) was on the spatiotemporal fractal aggregation of sawdust particles. Further, while the current paper demonstrates an easy method for the prediction of the location of sawdust particles with increasing time, the paper by Salau and Oke (2010) showed interest in health impairment of the complex aggregation of toxic sawdust particles. Also, the deterministic second order differential governing equation for Duffing's Oscillator is core to the current paper, while the paper by Salau and Oke (2010) was based on weighted random application of rules governing the motion of sawdust particles. The use of fractal principles in the formulation of sawdust particles is another way of solving similar problems of particle motion.

5.3 Application

Duffing's equation has been applied to the movement of sawdust particles. The results obtained can be used to predict the displacement and velocities of sawdust particles emitted in a saw mill. The work in this paper therefore, lays a foundation whereby practical data such as wind velocity, temperature variation in sawmills, wind forces, particle density, shape, and humidity can in future be used in refining the predictive capacity of the model developed here and therefore assist in locating particular sawdust particles in terms of their displacement and speed. With a model involving the parameters mentioned above, values could be fitted into the model to verify conformance to desired model results. Comparison of these parameters of velocity and displacement can also be done using the model developed in this work, for two or more particles in future investigations towards improving our understanding of emission parameters of various particles in the working environment, including sawdust, cement, and wool products.

Apart from the general theoretical models for predicting the emission characteristic of particles that have been presented in the work, models of sawdust emission include; Using the results in Srinivasakannan and Subramanian (2008), which investigated the size of sawdust in a Malaysian sawmill and defined it as being of an average of 2*mm* with 93% moisture content, the volume of sawdust accumulated around and away from the band saw could be calculated. This leads to the estimation of the distance that this volume of sawdust is away from the cutting point of the band saw through measurements. It is well known that velocity is the rate of change of displacement with time. Since time period could be read from each of the graphs (Figure 3 onward) a substitution of the unit of time would produce the distance that the sawdust particle is away from the band saw point of contact with the wood, although with multiple points because of the non-linearity and oscillatory characteristics of the motion.

UNIVERSITY OF IBADAN LIBRARY

6.0 CONCLUSIONS AND RECOMMENDATIONS

6.1 Conclusions

The main objective of this study was to understand the dynamic movement of sawdust particles after emission from sawmill machines, and to formulate a transformation that would enable a 2-dimensional graphical representation of the sawdust particle dynamic system in time series for the purpose of predicting its long term behaviour. The objective of the paper was achieved by first establishing the relevance of the harmonic function to modelling the possible patterns of movements of sawdust particles emitted from band saws, obtained through graphical transformation. This functional behavioural pattern is an inherent component of Duffing's equation, which was applied to the sawdust movement in sawmills using sawdust parameters from the literature. This utilised sawdust parameters of displacement, velocity and size. The displacement of the sawdust particles is in terms of its distance away from the source, band saw. The velocity of motion of sawdust over time was also reported. However, from literature sources, the size of sawdust was determined. A linear transformation was then superimposed on the Duffing system to permit proper observation of the predicted values of the motion of sawdust. With this, the much higher cost incurred through the traditional approach of collecting information of time history is avoided. This cost obtained through intuition and real cost is difficult to quantify.

The following basic conclusions can be drawn from the results of this work:

- The infinite continuous time series graph of a sawdust particle in the motion of a dynamic system can be compactly represented on a finite 2-D Euclidean dimension without loss of value. This has been explicitly demonstrated for the sawdust particle motion during emissions from the cutting operations.
- The required transformation may be improved upon. In addition to enabling reading of any desired value of the time series, the resulting 2-D transformation has the potential of differentiating periodic and chaotic dynamic systems in the movement of sawdust.
- The deficiency of the 2-D transformation is that when compared with phase plots as an analytical tool for dynamic systems, the system fixed/equilibrium points are not discernable on the 2-D transformation plane of the time series for the motion of sawdust particles.

6.2 Recommendations

- Further research may be able to establish the potential of the 2-D graphical representation as a predicting tool for the value of discrete time series such as the problem studied. The unique application of this future research to sawdust particle movement would be an important contribution to knowledge.
- In addition, an important future direction of research is to conduct a field scale case study through which some practical insights of the application of the model developed here to real-life situations can be obtained. In its present state, this paper ignores certain aspects of the real life possible applications of the model; this work considers the aspects of wind strength and humidity as negligible factors that would influence the model, which may not be so in real life situations. The fabrication and use of some of the required equipment may help to obtain results. For example, local manufacture of wind speed measuring device could be made to reduce cost.
- A future paper may cover application and practicability of the mathematical model developed here, with issues relevant to the model assumptions, limitations and application field discussed. Assumptions such as normal atmospheric conditions of temperature (room air temperature, 37°C) in the production of sawdust particles may be relaxed in further studies to take care of other variant conditions in real life.
- Proper quality control of raw material, wood, is the proper and accepted practice expected from activities in sawmills, as wood must have been checked and certified okay before usage. However, if the wood is defective, then the characteristic weight of the sawdust particle and its behaviour during wood production may be at variance from the normal. Future studies may consider the presence of wind energy, for instance, and how it would affect the displacement and velocity aspects of the model developed here.
- Wood types and classes such as soft and hardwoods need to be experimented on, as they may produce emitted sawdust that will show different behavioural patterns due to their different densities. Such variations are likely to affect the model and should be well accounted for in future research.
- Although it is concluded that the motion of the particles modelled is uncontrolled, however, there are several problems that relate to this type of motion and solutions may be suggested to them. Air is a principal problem. For example, as the wind ploughs, the motion of the sawdust particles may change, depending on the velocity of the wind. This may direct the particle to an undesired direction. The problem could be solved using wind breakers in the environment (i.e. tree planting has been found as an effective wind breaker). Also, work could be performed in an enclosure.

UNIVERSITY OF IBADAN LIBRARY

REFERENCES

1. Ahmad, B., Alsaedi, A., Aighamdi, B.S., "Analytic Approximation of Solutions of the Forced Duffing Equation with Integral Bounding Conditions", *Nonlinear Analysis: Real World Applications*, Vol. 9, 2008, pp. 1727-1740.
2. Ahmad, B., Aighamdi, B.S., "Approximation of Solutions of the Nonlinear Duffing Equation involving both Integral and Non-Integral Forcing Terms with Separated Boundary Conditions", *Computer Physics Communication*, Vol. 179, 2008, pp. 409-416.
3. Ahmad, B., Alsaedi, A., "Existence of Approximate Solution of the Forced Duffing Equation with Discontinuous Type of Integral Boundary Conditions", *Nonlinear Analysis: Real World Applications*, Vol. 10, 2009, pp. 358-367.
4. Arif, A.A., Delclos, G.L., Whitehead, L.W. and Tortolero, E.S.L., "Occupational Exposures Associated with Work-Related Asthma and Work-Related Wheezing Among U.S. Workers", *American Journal of Industrial Medicine*, Vol. 44, No. 4, 2003, pp. 368–376.
5. Baker G.L. and Gollub J.P., "Chaotic Dynamics: An Introduction", Cambridge University Press, Cambridge, New York, USA, 1990.
6. Bello S. R. and Mijinyawa Y. "Assessment of Injuries in Small Scale Sawmill Industry of South Western Nigeria", Agricultural Engineering International: CIGR Journal, Vol. 12, No. 1, 2010, pp. 151 –157.
7. Demers, P.A., Teschke, K. and Kennedy, S.M., "What to do about Softwood? A Review of Respiratory Effects and Recommendations Regarding Exposure Limits", *American Journal of Industrial Medicine*, Vol. 31, No. 4, 1997, pp. 385–398..
8. Dowell E., "Chaotic Oscillations in Mechanical Systems", *Computer and Structures*, Vol. 30, No. 1-2, 1988, pp. 171-184.
9. Gleick J., "Chaos: Making a New Science", Penguin Books, New York, USA, 1987.
10. Hamadi, N.K., Chen, X.D., Farid, M.M. and Lu, M.G.Q. "Adsorption Kinetics for the Removal of Chromium (VI) from Aqueous Solution by Adsorbents Derived from used Tyres and Sawdust", *Chemical Engineering Journal*, Vol. 81, No. 5, 2001, pp. 95–105,
11. Hamdaoui, Q., "Dynamic Sorption of Methylene Blue by Cedar Sawdust and Crushed Brick in Fixed Bed Columns", *Journal of Hazardous Materials*, Vol. 138, No. 2, 2006, pp. 293–303.
12. Heacock, H., Hertzman, C., Demers, P.A., Gallagher, R., Hogg, R.S., Teschke, K., Hershler, R., Bajdik, C.D., Dimich-Ward, H., Marion, S.A., Ostry, A., and Kelly, S., "Childhood Cancer in the Offspring in Male Sawmill Workers Occupationally Exposed to Chlorophenate Fungicides", *Environmental Health Perspectives*, Vol. 108, 2000, pp. 499–503.
13. Jadhav, D.N. and Vanjara, A.K., "Removal of Phenol from Wastewater using Sawdust, Polymerized Sawdust and Sawdust Carbon", *Indian Journal of Chemical Technology*, Vol. 11, No. 1, 2004, pp. 35–41.
14. Moon F.C., "Chaotic Vibrations: An Introduction for Applied Scientists and Engineers", John Wiley & Sons, Inc., New York, 1987.
15. Pier, P.A., Kelly, J.M., "Measured and Estimated Methane and Carbon Dioxide Emissions from Sawdust Waste in The Tennessee Valley under Alternative Management Strategies", *Bioresource Technology*, Vol. 61, 1997, pp. 213-220.
16. Salau T.A.O., Oke S.A., "Fractal Dimension and Time Factors of Sawdust Pattern Formation in Sawmills", *International Journal of Bio-inspired Computation*, Vol. 2, No. 2, 2010, pp. 142-150.
17. Šæiban, M., Klašnja, M. and Škrbiæ, B. "Modified Softwood Sawdust as Adsorbent of Heavy Metal ions from Water", *Journal of Hazardous Materials*, Vol. 136, No. 2, 2006, 266–271.
18. Siracusa, A., Kennedy, S.M., Dybuncio, A., Lin, F.J., Marabini, A. and Chan-Yeung, M., "Prevalence and Predictors of Asthma in Working Groups in British Columbia", *American Journal of Industrial Medicine*, Vol. 128, No. 3, 2007, pp. 411–423.
19. Srinivasakannan C., Subramanian N.B., "Drying Kinetics of Saw Dust in Tray Dryer", Journal of Sustainable Development, Vol. 1, No. 3, 2008, pp. 123-127.
20. Svedberg, U.R., Hogberg, H-E., Hogberg, J. and Galle, B. "Emission of Hexanal and Carbon Monoxide from Storage of Wood Pellets, a Potential Occupational and Domestic Health Hazard", *Annals of Occupational Hygiene*, Vol. 48, No. 4, 2004, pp. 339–349.
21. Taty-costodes, V.C., Fauduet, H., Porte, C. and Delacroix, A. "Removal of Cd(II) and Pb(II) ions, from Aqueous Solutions, by Adsorption onto Sawdust of Pinus Sylvestris', *Journal of Hazardous Materials*, Vol. 105, No. (1–3), 2003, pp. 121-142.
22. Zhang, W., Xiang B., "A Duffing Oscillator Algorithm to Detect the Weak Chromatographic Signal", *Analytical Chemical Acta*, Vol. 58, 2007, pp. 55-59.

UNIVERSITY OF IBADAN LIBRARY

APPENDIX-I TRANSFORMATION OF TRIGONOMETRIC FUNCTIONS

C. Transformation of Trigonometric function

```
      Implicit real *8(a-h,o-z)
      Open(unit=2,file='Timeseries')
      Open(unit=3,file='Timeseries.out')
      Pi2=6.0*acos(0.5)
      Write(*,*)'Wf,Nslice'
      Read(*,*)Wf,Nslice
      Fw=wf/pi2
      TP=1.0/fw
      Deltat=Tp/float(Nslice-1)
      write(*,*)mod(tp,pi2),tp
      Deltat6=Deltat/6.0
      Write(*,*)'Enter No of cycles to be examine'
      Read(*,*)NS
      Tt=0
      Itt=0

      Xdmin=1000
      Xvmin=Xdmin

C... The Real Experiments
      Do 20 I1=1,Ns
      Do 20 Jj=1,Nslice
      TT=tt+deltat
      X1=Cos(wf*tt)
      Y1=Sin(wf*tt)
C... The next if statement ensure stable results are reported!

      Write(2,26)wf*Tt,x1,y1
      Itt=Itt+1

      If(x1.lt.xdmin)xdmin=x1
      If(y1.lt.xvmin)xvmin=y1

 20   Continue
      Close(2)
      Open(unit=2,file='Timeseries')

      Write(*,*)'Xdmin and Xvmin are',xdmin,xvmin

      Xdmin=abs(xdmin)
      Xvmin=abs(xvmin)
   Do 30 i=1,itt
      Read(2,26)Tt,x1,y1
      Tita=mod(tt,pi2)
      Xd=(x1+xdmin)*cos(tita)
      Yd=(x1+xdmin)*sin(tita)
      Xv=(y1+xvmin)*cos(tita)
      Yv=(y1+xvmin)*sin(tita)
      Write(3,27)xd,yd,xv,yv
 30   Continue
 26   Format(3(f12.7,2x))
 27   Format(4(f10.5,2x))
      Stop
      End
```

UNIVERSITY OF IBADAN LIBRARY

APPENDIX-II TRANSFORMATION OF DUFFING'S SOLUTIONS

```
C. The Phase plot of Duffing system and Transformation of
C..both displacement and velocity components.
C..Transform linearly Displacement and velocity to ensure that
C..entries for transformation are all positive.
      Implicit real *8(a-h,o-z)
      Dimension x1(2),x2(2),Rt(4),Rk(4),Rg(4),Rf(4)
      Open(unit=1,file='Masterhomework.out')
      Open(unit=2,file='Timeseries')
      Open(unit=3,file='Timeseries.out')
      Pi2=6.0*acos(0.5)
      Write(*,*)Pi2
      Write(*,*)'Enter Damping Coefficient Heavy or Low'
      Read(*,*)Dampf
      Write(*,*)'Enter Initial conditions and Po,wf,Nslice'
      Read(*,*)x1(1),x2(1),Po,wf,Nslice
      Fw=wf/pi2
      TP=1.0/fw
      Deltat=Tp/float(Nslice-1)
      Deltat6=Deltat/6.0
      Write(*,*)'Enter No of Run away cycles and to be examine'
      Read(*,*)Ns,Ne
      Tt=0
      Itt=0
      Xdmin=1000
      Xvmin=Xdmin
C... The Real Experiments
      Do 20 I1=1,NE+Ns
   Do 20 I2=1,Nslice
      Rt(1)=tt
      Rt(2)=TT+deltat*0.5
      Rt(3)=Rt(2)
      Rt(4)=Rt(1)+deltat
      Do 15 I=1,4
      If(i.eq.1)then
      Rk(i)=x1(1)
      Rg(i)=x2(1)
      Else
      If(i.eq.4)then
      Rk(i)=x1(1)+deltat*Rg(i-1)
      Rg(i)=x2(1)+deltat*Rf(i-1)
      Else
      Rk(i)=x1(1)+Rg(i-1)*deltat*0.5
      Rg(i)=x2(1)+Rf(i-1)*deltat*0.5
      Rf(i)=Po*cos(wf*Rt(i))+Rk(i)-0.5*(Rk(i)**3)-Dampf*Rg(i)
      Endif
      Endif
15    Continue
      X1(2)=x1(1)+deltat6*(Rg(1)+2.0*(Rg(2)+Rg(3))+Rg(4))
      X2(2)=x2(1)+deltat6*(Rf(1)+2.0*(Rf(2)+Rf(3))+Rf(4))
      TT=Rt(4)
C... The next if statement ensure stable results are reported!
      If(I1.gt.Ns)then
      Write(1,25)x1(2),x2(2)
      Write(2,26)wf*Tt,x1(2),x2(2)
      Itt=Itt+1
      If(x1(2).lt.xdmin)xdmin=x1(2)
      If(x2(2).lt.xvmin)xvmin=x2(2)
      Endif
```

UNIVERSITY OF IBADAN LIBRARY

```
      x1(1)=x1(2)
      x2(1)=x2(2)
20  Continue
      Close(2)
      Open(unit=2,file='Timeseries')
      Write(*,*)'Xdmin and Xvmin are',xdmin,xvmin
      Xdmin=abs(xdmin)
      Xvmin=abs(xvmin)
   Do 30 i=1,itt
      Read(2,26)Tt,x1(2),x2(2)
      Tita=mod(tt,pi2)
      Xd=(x1(2)+xdmin)*cos(tita)
      Yd=(x1(2)+xdmin)*sin(tita)
      Xv=(x2(2)+xvmin)*cos(tita)
      Yv=(x2(2)+xvmin)*sin(tita)
      Write(3,27)xd,yd,xv,yv
30    Continue

25    Format(2(f10.5,2x))
26    Format(3(f12.7,2x))
27    Format(4(f10.5,2x))
      Stop
      End
1.  2000.
```

UNIVERSITY OF IBADAN LIBRARY

 © KJME 2010